Journal of Alloys and Compounds 580 (2013) S47–S50

Contents lists available at SciVerse ScienceDirect

Journal of Alloys and Compounds

journal homepage: www.elsevier.com/locate/jalcom

Mapping trends in the reorientational mobilities of tetrahydroborate anions via neutron-scattering fixed-window scans

Terrence J. Udovic [a,*], Nina Verdal [a,b], John J. Rush [a,b], Daniel J. De Vries [c], Michael R. Hartman [d], John J. Vajo [e], Adam F. Gross [e], Alexander V. Skripov [f]

[a] NIST Center for Neutron Research, National Institute of Standards and Technology, 100 Bureau Dr., MS 6102, Gaithersburg, MD 20899-6102, USA
[b] Department of Materials Science and Engineering, University of Maryland, College Park, MD 20742-2115, USA
[c] Radiation and Isotopes for Health, Delft University of Technology, Mekelweg 15, 2629 JB Delft, Netherlands
[d] Nuclear Engineering and Radiological Sciences, University of Michigan, Ann Arbor, MI 48109-2104, USA
[e] HRL Laboratories, LLC, 3011 Malibu Canyon Road, Malibu, CA 90265, USA
[f] Institute of Metal Physics, Ural Division of the Russian Academy of Sciences, S. Kovalevskoi 18, Ekaterinburg 620041, Russia

ARTICLE INFO

Article history:
Available online 19 February 2013

Keywords:
Energy storage materials
Diffusion
Inelastic neutron scattering

ABSTRACT

The reorientational dynamics of tetrahydroborate (BH_4^-) anions in a variety of environments were probed as a function of temperature via fixed-window scans (FWSs) at zero energy transfer using a neutron backscattering spectrometer. The temperature dependence of the FWS was shown to be a sensitive indicator of the relative reorientational mobilities of BH_4^- anions in the various alkali-metal borohydride compounds MBH_4 (M = Li, Na, K, Rb, Cs), $LiBH_4$ nanoconfined in carbon aerogel, and $LiBH_4$–LiI solid solution.

Published by Elsevier B.V.

1. Introduction

Metal borohydrides are one class of materials under intense scrutiny as potential hydrogen-storage materials [1]. The nature of the tetrahydroborate (BH_4^-) anion environment in metal borohydrides due to cation type, nanoconfinement, and interactions with different chemical constituents may result in significant changes in the BH_4^- reorientational potential landscapes, which can be followed by a variety of experimental techniques, such as vibrational spectroscopies [2–7], NMR [8–13], and quasielastic neutron scattering (QENS) [5,14–18]. The latter is particularly sensitive and useful for studying the dynamics of BH_4^- (or other hydrogenous species) due to the relatively large hydrogen incoherent neutron scattering cross section and the fact that BH_4^- anions undergo sufficiently rapid reorientational motions to be observable within the neutron time window ($\approx 10^{-13}$–10^{-8} s, depending on the spectrometer). In a quasielastic neutron scattering experiment, a portion of the incident neutrons interact with the hydrogen nuclei of the reorienting BH_4^- anions and become Doppler-broadened. The resulting scattering spectrum centered at zero energy transfer possesses both an elastic component (delta function) reflecting the overall localization of the BH_4^- anions, and a broader quasielastic component (one or more Lorentzian functions) reflecting the reorienting BH_4^- anions (i.e., H rotational motions around the "stationary" B atoms). Both components are convoluted with the (typically Gaussian) instrumental resolution function. In general, the width of the quasielastic component is a measure of the reorientational jump rate; i.e., the wider the component, the larger the jump rate.

A useful QENS measurement that is typical of, but by no means exclusive to, the neutron backscattering spectrometer is the so-called fixed-window scan (FWS). In the FWS, only elastically scattered (i.e., zero-energy-transfer) neutrons are measured from the sample as a function of temperature. At very low temperatures, the rate of reorientational motion will be too low and thus the quasielastic component too narrow to be separable from the resolution-broadened, purely elastic component. In this case, the elastic and quasielastic components are indistinguishable and additive, maximizing the number of scattered neutrons in the FWS. In contrast, at very high temperatures, the rate of reorientational motion will be too high, yielding a quasielastic component that is much broader than the energy range of the instrument. In this case, the quasielastic component collapses and contributes no significant intensity at zero energy transfer to that of the elastic component in the FWS. At intermediate temperatures, the rate of reorientational motion results in observable quasielastic scattering intensity at zero energy transfer, leading to "intermediate" intensities in the FWS. Thus, from a typical FWS shown schematically in Fig. 1, one is able to define, from the drop in signal, the temperature range for which the BH_4^- reorientation rate is within the neutron time window of the spectrometer. By comparing FWSs of BH_4^- anions in different samples, one can determine among other things, the

* Corresponding author. Tel.: +1 301 975 6241; fax: +1 301 921 9847.
E-mail address: udovic@nist.gov (T.J. Udovic).

0925-8388/$ - see front matter Published by Elsevier B.V.
http://dx.doi.org/10.1016/j.jallcom.2013.02.025

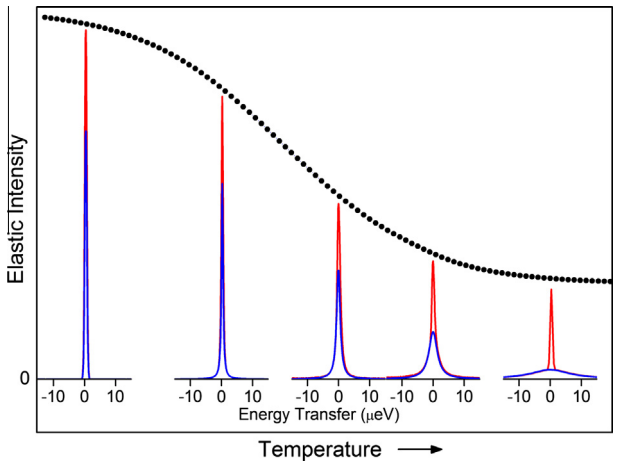

Fig. 1. A typical fixed-window scan at zero energy transfer (closed circles), showing the effect of the temperature-dependent broadening of the quasielastic component (blue line) on the overall neutron scattering spectrum (red line). (For interpretation of the references to colour in this figure legend, the reader is referred to the web version of this article.)

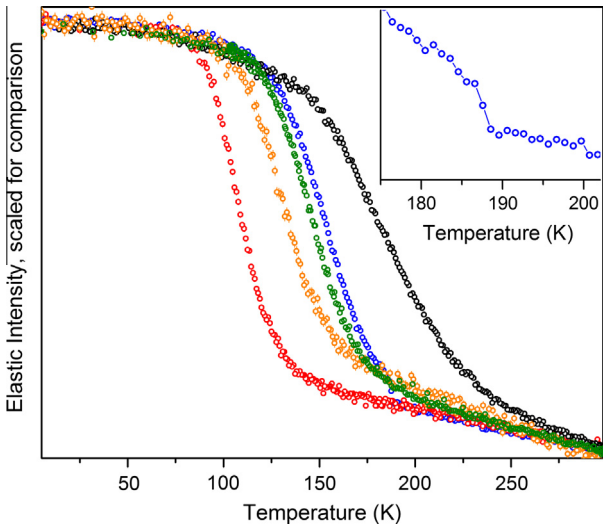

Fig. 2. Fixed-window scans for BH_4^- anions in MBH_4 compounds (from right to left, M = Li, Na, K, Rb, and Cs) as a function of temperature. The inset shows FWS evidence of the order–disorder phase transition of $NaBH_4$ just below 190 K.

order of reorientation rates at a given temperature as well as the temperatures at which each possess a similar reorientation rate.

In this paper, we demonstrate the utility of the FWS for assessing the relative reorientational mobilities of BH_4^- anions in various solid-state environments, namely in the alkali-metal borohydrides MBH_4 (M = Li, Na, K, Rb, Cs), $LiBH_4$ nanoconfined in carbon aerogel, and $LiBH_4$–LiI solid solution.

2. Experimental details

To avoid neutron absorption problems, all borohydride samples were ^{11}B-enriched, and $LiBH_4$ samples were also ^7Li-enriched. Details of borohydride sample syntheses are reported elsewhere [3,5,7]. Carbon aerogels with 13 nm average pore size were synthesized using resorcinol–formaldehyde condensation, as detailed elsewhere [19] followed by vacuum drying overnight at 630 K. $LiBH_4$ was incorporated into the aerogel pores by melt infiltration under 1 bar of H_2. Two samples were prepared, one completely filled and one partially filled (22%) with $LiBH_4$. The pore fill fractions were confirmed via cold-neutron prompt-gamma activation analysis (PGAA) [20] at NG-7 [21] at the NIST Center for Neutron Research (NCNR). The $LiBH_4$–LiI solid solution was formed by ball-milling together equal molar amounts of $LiBH_4$ and LiI as in Ref. [22] and subsequently annealing for 4 d at 523 K in an inert environment. (The partial I^- substitution of BH_4^- anions is known to stabilize the hexagonal structure of the high-temperature $LiBH_4$ phase down to low temperatures [8,12].) All powder samples were loaded in Al cans in annular geometry, resulting in ≈10% scatterers. All FWS measurements were performed at the NCNR on the High-Flux Backscattering Spectrometer (HFBS) [23]. For a direct comparison, the FWSs were formed by the summation of all HFBS detectors and scaled appropriately to match all the intensities at the lowest and highest temperatures.

3. Results and discussion

Fig. 2 displays the FWSs for the family of alkali-metal borohydrides between 4 K and 300 K. Although in this temperature range, the orthorhombic structure for $LiBH_4$ is atypical of the face-centered-cubic structure observed for $NaBH_4$, KBH_4, $RbBH_4$, and $CsBH_4$, its FWS indicates that it possesses the least rotationally-mobile BH_4^- anions of all alkali-metal analogs, which is in line with the overall observed trend in Fig. 2 that mobility increases with cation size. The onset temperatures of observable motion (on the order of 10^8 jumps/s for the HFBS) are approximately 150 K for $LiBH_4$, 120 K for $NaBH_4$ and KBH_4, 100 K for $RbBH_4$, and 80 K for $CsBH_4$. Likewise, the temperatures where motion starts becoming too rapid (surpassing 10^{10} jumps/s for the HFBS) to be easily observed are approximately 270 K for $LiBH_4$, 200 K for $NaBH_4$ and KBH_4, 190 K for $RbBH_4$, and 170 K for $CsBH_4$.

The inset in Fig. 2 shows the sensitivity of the FWS to the subtle order–disorder transition for $NaBH_4$ that occurs within the neutron time window near 190 K. In particular, there is a distinct step change in the FWS upon crossing the transition. This indicates that the BH_4^- anions in the orientationally ordered phase undergo a step increase in their reorientation rate upon transformation to the orientationally disordered phase.

Fig. 3 displays the FWSs for $LiBH_4$ in different environments; in particular, bulk $LiBH_4$, $LiBH_4$ (completely filled) in carbon aerogel, $LiBH_4$ (partially filled, 22%) in carbon aerogel, and a 1:1 $LiBH_4$–LiI solid solution. The completely filled aerogel displays a FWS somewhat similar to that for bulk $LiBH_4$. The only difference appears to be an earlier onset temperature near 100–110 K for some small fraction of more mobile BH_4^- anions. This suggests that a significant fraction of the $LiBH_4$ in the aerogel possesses bulk-like behavior. In contrast, the FWS for $LiBH_4$ in the partially filled aerogel is clearly showing much more mobile, non-bulk-like behavior. In this

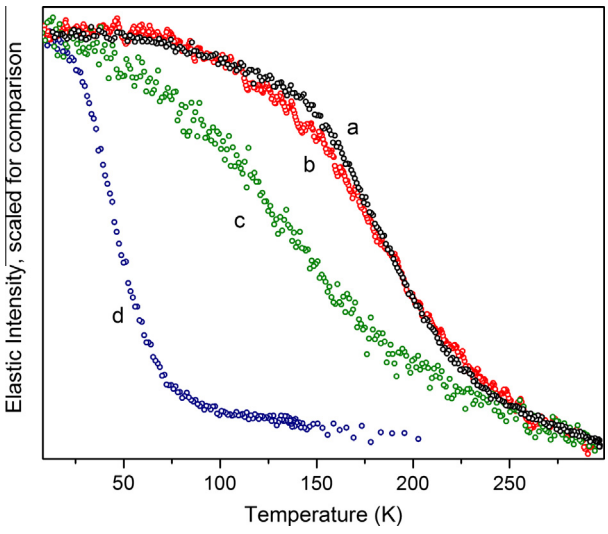

Fig. 3. Fixed-window scans as a function of temperature for BH_4^- anions in (a) bulk $LiBH_4$, (b) $LiBH_4$ (completely filled) in a 13 nm carbon aerogel, (c) $LiBH_4$ (partially-filled, 22%) in a 13 nm carbon aerogel, and (d) a 1:1 $LiBH_4$–LiI solid solution.

case, there appears to be a distribution of BH_4^- mobilities (i.e., a wider temperature range within the neutron time window) with a much lower onset temperature near 40–50 K for the more mobile anions.

The differences between the two aerogel samples strongly suggest that the $LiBH_4$ in the partially (22%) filled sample preferentially infiltrated the smallest pores. (N.B., the micropore/mesopore volume ratio for the 13 nm aerogel was 0.18 [19], meaning that the smaller micropores comprise about 15% of the pore volume, only slightly smaller than the 22% fill fraction.) Indeed, previous NMR studies [9] have suggested that the BH_4^- anions associated with $LiBH_4$ near the pore interfaces of the carbon aerogel are much more mobile than those associated with the more bulk-like $LiBH_4$ in the interior of the pore, away from the pore interfaces. This may be due to a combination of fewer anion and cation neighbors (lower coordination) for anions next to the interface and weaker interactions between these anions and the interfacial carbon atoms. For smaller pores, the fraction of more mobile interface BH_4^- anions increases, as suggested by the FWS. If we assume that there are roughly two types of BH_4^- anions in the nanopores, more mobile interface anions and less mobile interior bulk-like anions, then the total FWS will be the summation of separate FWSs associated with each type of anion: an "interface" component significantly downshifted in temperature (by around 100 K compared to bulk $LiBH_4$) and an "interior" component exhibiting bulk-like behavior. The combination would yield a total FWS close to what is observed. As for the completely filled aerogel, since the 13 nm carbon aerogel is known to have a rather broad distribution of pore sizes with a dominant volume fraction of the larger mesopores [19], there is necessarily a much larger fraction of $LiBH_4$ in the larger pores. Hence, the fraction of "interior" $LiBH_4$ is much larger than for the partially filled aerogel, resulting in a FWS reflecting more bulk-like behavior.

Finally, the FWS for the $LiBH_4$–LiI solid solution sample indicates that the BH_4^- anions are by far the most reorientationally mobile of the samples measured, with an onset temperature below 30 K followed by a sharp drop-off and exiting the neutron time window by around 90 K. This is in agreement with the known enhanced mobility observed previously by NMR and QENS measurements [12,16]. This extremely high mobility reflects the abnormally large BH_4^- crystallographic site in the hexagonal $LiBH_4$–LiI lattice, coupled with the rather weak rotational potential for the BH_4^- anions presumably around the *c*-directed trigonal axis as observed previously for hexagonal $LiBH_4$ [18].

For the sake of simplicity, we have assumed in all our analyses above that the BH_4^- reorientational mechanism is the same for each compound, which is not necessarily true (although for the compounds in Fig. 2, it is not an unreasonable assumption). One should at least be aware that drastically different mechanisms may lead to somewhat different temperature-dependent contours for the FWSs. This is because the fraction of elastic scattering compared to the total elastic + quasielastic scattering (even if averaged over the momentum-transfer range of the instrument) is mechanism-dependent [5]. For example, a BH_4^- reorientational mechanism involving uniaxial 120° jumps around a single B–H axis will result in a larger fraction of elastic scattering than one involving tetrahedral tumbling of H atoms among all four H sites [18]. Also, the contour can be perturbed if the mechanism happens to change with temperature across the FWS. Some of these potential complications are mitigated by the rescaling of the FWSs to normalize the minima and maxima. Moreover, even if different mechanisms are involved, this only affects the shape of the FWS drop-off region; it does not weaken our analyses concerning the onset temperatures, the implied distributions of BH_4^- environments, and the relative ranking of mobilities among samples.

4. Conclusions

In this paper, we have demonstrated the utility of neutron-scattering fixed-window scans for mapping trends in BH_4^- mobilities subjected to different solid-state environments. Of course, this type of measurement is not restricted to BH_4^- reorientations. Any localized motion of hydrogen or hydrogen-containing groups can be mapped out, such as has been shown for characterizing the motions of interstitial hydrogen in metals [24], the reorientational mobility of the larger $(B_{12}H_{12})^{2-}$ icosahedral anion in $Cs_2B_{12}H_{12}$ [25], or the dynamics associated with macromolecular systems [26]. Moreover, in general, there is more information that can be extracted from the functional form of the FWS, such as an estimate of the activation energy for reorientation, but this requires plotting the FWS at a particular momentum transfer combined with some knowledge of the reorientation mechanism [27], which is beyond the intent of this paper. The primary function of the FWS is typically to assess the temperature regime where hydrogen-related mobilities are within the neutron time window of the spectrometer. This information can guide more extensive quasielastic neutron scattering measurements of intensity versus energy transfer at various temperatures to more rigorously determine the mechanism and activation energy for reorientation. It is obvious though, that even without these more extensive measurements, the FWS can provide simple yet important comparative insights concerning the mobilities of reorienting moieties in technologically important materials.

Acknowledgements

This work was partially supported by DOE-EERE under Grant Nos. DE-AI-01-05EE11104, DE-EE0002978, and DE-FC36-05GO15067. This work utilized facilities supported in part by the National Science Foundation under Agreement DMR-0944772. This work was also partially supported by the Russian Foundation for Basic Research under Grant No. 12-03-00078.

References

[1] V. Stavila, L. Klebanoff, J. Vajo, P. Chen, in Hydrogen Storage Technology: Materials and Applications (L. Klebanoff, Ed.), CRC Press, Boca Raton, 2012, pp. 133–211.
[2] H. Hagemann, S. Gomes, G. Renaudin, K. Yvon, J. Alloys Comp. 363 (2004) 126.
[3] M.R. Hartman, J.J. Rush, T.J. Udovic, R.C. Bowman, S.-J. Hwang, J. Sol. State Chem. 180 (2008) 1298.
[4] H. Hagemann, Y. Filinchuk, D. Chernyshov, W. van Beek, Phase Transitions 82 (2009) 344.
[5] N. Verdal, M.R. Hartman, T. Jenkins, D.J. DeVries, J.J. Rush, T.J. Udovic, J. Phys. Chem. C 114 (2010) 10027.
[6] A. Borgschulte, A. Jain, A.J. Ramirez-Cuesta, P. Martelli, A. Remhof, O. Friedrichs, R. Gremaud, A. Züttel, Faraday Discuss. 151 (2011) 213.
[7] N. Verdal, T.J. Udovic, W. Zhou, J.J. Rush, D.J. De Vries, M.R. Hartman, J. Phys. Chem. C 117 (2013) 876.
[8] H. Maekawa, M. Matsuo, H. Takamura, M. Ando, Y. Noda, T. Karahashi, S.-I. Orimo, J. Amer. Chem. Soc. 131 (2009) 894.
[9] D.T. Shane, R.L. Corey, C. McIntosh, L.H. Rayhel, R.C. Bowman Jr., J.J. Vajo, A.F. Gross, M.S. Conradi, J. Phys. Chem. C 114 (2010) 4008.
[10] A.V. Skripov, A.V. Soloninin, O.A. Babanova, J. Alloys Comp. 509S (2011) S535.
[11] K. Jimura, S. Hayashi, J. Phys. Chem. C 116 (2012) 4883.
[12] A.V. Skripov, A.V. Soloninin, L.H. Rude, T.R. Jensen, Y. Filinchuk, J. Phys. Chem. C 116 (2012) 26177.
[13] M.H.W. Verkuijlen, P. Ngene, D.W. de Kort, C. Barré, A. Nale, E.R.H. van Eck, P.J.M. van Bentum, P.E. de Jongh, A.P.M. Kentgens, J. Phys. Chem. C 116 (2012) 22169.
[14] A. Remhof, Z. Łodziana, P. Martelli, O. Friedrichs, A. Züttel, A.V. Skripov, J.P. Embs, T. Strässle, Phys. Rev. B 81 (2010) 214304.
[15] D. Blanchard, M.D. Riktor, J.B. Maronsson, H.S. Jacobsen, J. Kehres, D. Sveinbjörnsson, E.G. Bardají, A. Léon, F. Juranyi, J. Wuttke, B.C. Hauback, M. Fichtner, T. Vegge, J. Phys. Chem. C 114 (2010) 20249.
[16] P. Martelli, A. Remhof, A. Borgschulte, R. Ackermann, T. Strässle, J.P. Embs, M. Ernst, M. Matsuo, S.-I. Orimo, A. Züttel, J. Phys. Chem. A 115 (2011) 5329.
[17] D. Blanchard, J.B. Maronsson, M.D. Riktor, J. Kheres, D. Sveinbjörnsson, E.G. Bardají, A. Léon, F. Juranyi, J. Wuttke, K. Lefmann, B.C. Hauback, M. Fichtner, T. Vegge, J. Phys. Chem. C 116 (2012) 2013.

[18] N. Verdal, T.J. Udovic, J.J. Rush, J. Phys. Chem. C 116 (2012) 1614; ibid. 116 (2012) 5275.
[19] A.F. Gross, J.J. Vajo, S.L. Van Atta, G.L. Olson, J. Phys. Chem. C 112 (2008) 5651.
[20] R.L. Paul, R.M. Lindstrom, J. Radioanal. Nucl. Chem. 243 (2000) 181.
[21] R.M. Lindstrom, J. Res. Natl. Inst. Stand. Technol. 98 (1993) 127.
[22] L.H. Rude, E. Groppo, L.M. Arnbjerg, D.B. Ravnsbæk, R.A. Malmkjær, Y. Filinchuk, M. Baricco, F. Besenbacher, T.R. Jensen, J. Alloys Comp. 509 (2011) 8299.
[23] A. Meyer, R.M. Dimeo, P.M. Gehring, D.A. Neumann, Rev. Sci. Instrum. 74 (2003) 2759.
[24] E. Mamontov, T.J. Udovic, O. Isnard, J.J. Rush, Phys. Rev. B 70 (2004) 214305.
[25] N. Verdal, T.J. Udovic, J.J. Rush, R.L. Cappelletti, W. Zhou, J. Phys. Chem. A 115 (2011) 2933.
[26] C.L. Soles, J.F. Douglas, W.-L. Wu, J. Polym. Sci. B: Polym. Phys. 42 (2004) 3218.
[27] M. Prager, H. Grimm, I. Natkaniec, D. Nowak, T. Unruh, J. Phys.: Condens. Matter 20 (2008) 125218.